Highly Directive 18.9 nm Nickel-like Molybdenum X-Ray Laser Operating at 150 mJ Pump Energy

T. Ozaki,[1] R. A. Ganeev,[1,2] A. Ishizawa,[1,2] T. Kanai,[1,2] and H. Kuroda[1,2]

[1]*NTT Basic Research Laboratories, NTT Corporation, 3-1 Morinosato Wakamiya, Atsugi, Kanagawa 243-0198, Japan*

[2]*Institute for Solid State Physics, University of Tokyo, 5-1-5 Kashiwanoha, Kashiwa, Chiba 277-8581, Japan*

(Received 1 August 2002; published 27 November 2002)

We experimentally demonstrate that by longitudinally pumping 2 mm long molybdenum preformed plasma with high-intensity 475 fs duration laser pulse, a highly directive soft-x-ray laser at 18.9 nm wavelength is generated. The divergence of the beam is evaluated to be of the submilliradian order, and only requires a pump laser energy of 150 mJ.

DOI: 10.1103/PhysRevLett.89.253902 PACS numbers: 42.55.Vc, 41.50.+h, 52.38.Dx

A major motivation for present-day x-ray-laser research is to show that this unique source is in fact useful. Application experiments of x-ray lasers were greatly accelerated by the development of a 4 Hz repetition-rate neonlike argon x-ray laser based on the capillary discharge-pumping method [1]. This efficient x-ray laser, with an average power of 3.5 mW and a beam divergence of 4.6 mrad [2], has been used in the determination of optical constants [3], characterization of diffraction gratings [4], as well as interferomic imaging of laser plasmas and pinch discharges [5–7]. Another popular scheme in present-day x-ray laser research is the transient-collisional-excitation (TCE) x-ray laser [8,9]. The TCE scheme has been successfully demonstrated by a number of groups throughout the world at various wavelengths, using both neonlike and nickel-like ions. In spite of its high reliability, one hurdle that must be cleared with this scheme is the improvement of the spatial coherence, which is limited by the short-length of the grain medium used with this scheme. Another difficulty of the TCE scheme is that multijoule pump laser energy is required for high-gain operation, which limits the repetition rate of this x-ray laser to one shot in every few minutes. It would therefore be exciting to think of the numerous fascinating areas of application that might be realized with the advent of TCE lasers in the soft-x-ray wavelength region, with high output energy, high spatial coherence, and operating at multihertz repetition rates.

In the present paper, we describe a TCE x-ray laser system that might possess the capability of opening a new phase in x-ray laser application. The 18.9 nm nickel-like molybdenum x-ray laser described in this paper has an extraordinary small divergence, and also operates with only 150 mJ pump laser energy. Li and co-workers first proposed this novel method [10], which was first experimentally demonstrated by Li and Xu [11] using tabletop Ti:sapphire laser pulses coupled into molybdenum capillary targets. The experimental results in the present work use slab molybdenum targets instead, and reveal an additional favorable characteristic of longitudinal-pumped TCE x-ray laser. We demonstrate ultrasmall divergence of less than 1 mrad using this scheme, with the spot size of the x-ray laser beam measured to be 90 μm at a distance of 270 mm from the source. The divergence of this 18.9 nm x-ray laser is less than 1 mrad, demonstrating that it is possible to obtain high spatial coherence even for short-length amplified spontaneous emission systems. The mechanism for realizing such high coherence is attributed to the selective amplification of low-order transverse modes, resulting from the refraction of high-order modes due to density and gain gradients generated by the pedestal of the main subpicosecond pump pulse.

Figure 1 shows the schematic of our experiment. A 2 mm long slab molybdenum target (T) is placed within a vacuum chamber, which is pumped by two laser beams from a tabletop 1.06 μm wavelength Nd:glass/Ti:sapphire hybrid chirped pulse amplification laser system [12]. First, the 300 ps duration prepulse is line focused onto the target surface using a cylindrical lens, which produces the highly ionized molybdenum preplasma. After a typical time of several nanoseconds, an intense 475 fs main pulse is point focused and pumps the preplasma from a longitudinal direction. The dimensions of the long pulse at focus are 100 μm wide and 2 mm long, and the spot diameter and confocal parameter of the

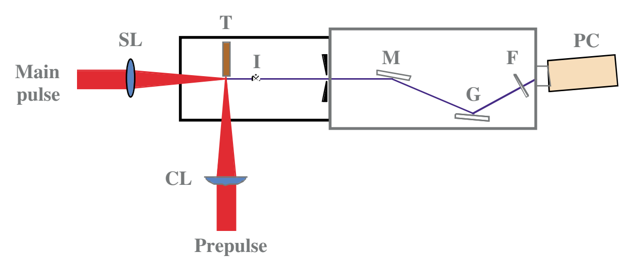

FIG. 1 (color online). Diagram of the experimental setup. The symbols shown in the figure correspond to spherical lens (SL), cylindrical lens (CL), molybdenum target (T), position that is spatially imaged onto the spectrometer focal plane (I), cylindrical gold-coated mirror (M), Hitachi flat-field grating (G), 0.65 μm thick Al foil (F), and photocathode camera (PC).

short pulse is 30 and 10 mm, respectively. Typical intensities of the long and short pulses are 1.5×10^{11} W cm^{-2} and 3×10^{16} W cm^{-2}, respectively. Using neutral density filters and fast-response photomultiplier tube, the contrast ratio between the pedestal and peak of the short pulse was measured to be 1×10^{-5}. The short pulse enters the preplasma at a position between 0.1 and 0.2 mm from the target surface, and the peak-to-peak delay time between the two pulses is varied between 1 and 10 ns. The on-axis soft-x-ray radiation is spectrally dispersed using a Hitachi 1200 lines/mm flat-field spectrograph, and the time-integrated soft x-ray spectrum is detected using a Hamamatsu C1936 photocathode camera. The planar photocathode of this camera is 30 nm thick gold coated on 100 nm thick parylene film. A gold-coated cylindrical mirror (M) is used to image x rays at position (I) in Fig. 1 onto the detector plane, with a magnification factor of unity. However, we set the target at a position that is 70 mm away from this imaging position, so that the divergence of the soft-x-rays in the direction vertical to the target surface could be evaluated. Additionally, the slit of the spectrometer, which is at a distance of 270 mm from the target, is opened to a width of 1.6 mm, in order to observe the divergence of the x-rays in the direction of spectral dispersion. The photon number reaching the detector is evaluated by comparing the signal from the spectrograph system with those from a commercial vacuum monochromator (Acton VM504) combined with a photomultiplier tube (Hamamatsu R2496) and a sodium salicylate coated window. Aluminum filters with thickness of 0.65 μm is used for both the Hitachi spectrograph and the Acton spectrometer, to eliminate strong visible emission from the plasma, including the high-intensity short pulse laser transmitted through the preplasma.

In Fig. 2 we show the intensity trace of a typical on-axis soft-x-ray spectrum between 15 and 25 nm observed using the above experimental setup. The pump laser energy in the long and short pulse is 30 and 120 mJ, respectively, and the peak-to-peak delay time between the two pulses is 4 ns. We can see from this figure that the on-axis emission from the molybdenum plasma is completely dominated by a single line at 18.9 nm, which is assigned the $3d^9 4d\ ^1S_0$–$3d^9 4p\ ^1P_1$ line of nickel-like molybdenum. The result shows that the spectral intensity of the continuum near the x-ray laser line is at the noise level. This can be inferred from the fact that a sharp cutoff at 17 nm cannot be seen in the spectrum, although 0.65 μm thick Al filters are used. This thus demonstrates the large ratio between the x-ray laser and continuum emission signals.

The most interesting point about the observed spectrum is the narrow spectral width of the 18.9 nm line, in spite of the fact that the spectrograph slit is widely opened to a width of 1.6 mm. In fact, the size of the 18.9 nm line at the detector plane is not only small in the direction of spectral dispersion, but also in the direction vertical to it. This can be seen in Fig. 3(a), which is the raw image of the on-axis spectrum between 16 and 22 nm wavelengths for 2 mm long molybdenum plasma. By fitting the observed intensity profile of the 18.9 nm line assuming a Gaussian transverse mode, the full width at $1/e^2$ maximum of this spot at the detector plane is 93 μm in the direction of spectral dispersion and 85 μm in the vertical direction.

From these dimensions, we can estimate the upper limit of the x-ray laser divergence observed in this work. In the present case, the size of the 18.9 nm line in the direction of spectral dispersion corresponds to the size of the x-ray laser at the spectrograph slit, since the width of the slit is widely opened to 1.6 mm. Since the distance between the source and the slit is 270 mm, we estimate the divergence in the direction parallel to the target surface to be 0.34 mrad. On the other hand, the size of the 18.9 nm spot in the direction normal to the target surface corresponds to the size of the x-ray laser at the imaging position (I) in Fig. 1. Therefore, the estimated divergence in the normal direction is smaller than

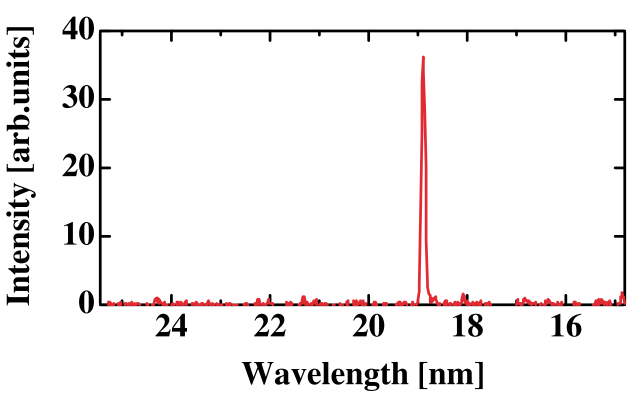

FIG. 2 (color online). Intensity trace of the on-axis soft-x-ray spectrum between 15 and 25 nm. The background was subtracted from the trace to obtain the actual intensity profile.

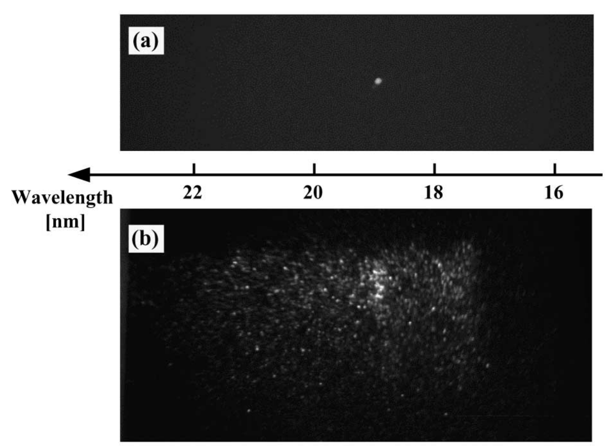

FIG. 3. Spectrum image of the on-axis emission for plasma lengths of (a) 2.0 mm and (b) 0.5 mm. The sensitivity of the photocathode camera was increased by about 8 times for (b).

1.2 mrad. The divergence of the present x-ray laser is a 1 order of magnitude improvement compared with past works, and combined with the small pump energy required, should prove to be a large merit for application experiments. We have also investigated the 18.9 nm x-ray divergence generated from preformed plasma with shorter lengths. In Fig. 3(b) we show the on-axis soft x-ray spectrum near the 18.9 nm line for prepulse laser with line-focus length of 0.5 mm. The result shows a great increase in the divergence of the 18.9 nm line for the shorter plasma, especially in the direction vertical to the target surface. The ratio between the 18.9 nm line and the continuum emission is greatly decreased compared with the two mm long plasma spectrum.

Because of the difficulty of determining gain coefficients in longitudinally pumped lasers, we measure the energy of 18.9 nm line to estimate the magnitude of amplification achieved in this work. After careful calibration of the Hitachi and Acton spectrometers, the typical energy of the 18.9 nm line is measured to be 27 nJ per pulse. This energy is 85 times smaller than that measured for saturated conventional, transversely pumped nickel-like molybdenum x-ray laser [13]. However, the dimension of the lasing region for the present work should be no larger than the spot size of the longitudinal pump beam, which is 30 μm in diameter. Therefore, the lower limit in the output energy fluence of the present 18.9 nm x-ray laser is 3.8 mJ cm^{-2}, which is 1 order of magnitude smaller than that demonstrated by Li *et al.* [13]. This estimation, along with the dominant 18.9 nm spectrum of Fig. 2, shows that the present x-ray laser is operated at large gain-length products, close to, but below the saturation level.

A big question arises as to why such highly directive x-ray lasers can be generated from short 2-mm-long plasma. We attribute this unique phenomenon to the presence of a 1×10^{-5} pedestal in the longitudinal pump beam. There are two outcomes of this pedestal that can greatly affect the divergence of the present x-ray laser. First is the localization of the nickel-like ion abundant region to the position of the longitudinal beam. Hydrodynamic simulations using the HYADES code [14] show that the electron density and temperature of the preplasma is 4×10^{19} cm^{-3} and 20 eV, respectively, at a position 100 μm from the target surface, and at a time 4 ns from the peak of the prepulse. In this case, the average ionization of the preplasma is 8, much less than 14 required for nickel-like molybdenum ions. However, by taking into account the pedestal of the main pulse, which has a peak intensity 2 times higher than that of the prepulse, the temperature and density of the region irradiated by the pedestal is increased. Simulations show that, for the present experimental condition, a region with a paraboliclike temperature and density profile is produced, with a peak temperature and density of 90 eV and 1×10^{20} cm^{-3}, respectively. As a result, a 35 μm wide nickel-like molybdenum abundant region is produced within the preplasma, which can generate high gain with the irradiation of the high-intensity main pump. To illustrate this effect, the result of gain calculation with the above pedestal condition is shown in Fig. 4. Here the pedestal produces a density profile within the prepulse-produced plasma in the x direction normal to the target surface, which is assumed to be uniform in the z direction parallel to the x-ray laser axis. We see that gain coefficients exceeding 70 cm^{-1} are generated at the entrance of the preplasma, over a length of 500 μm. A long and narrow positive gain region extends over the full length of the 2-mm-long preplasma, which corresponds to the region that is pumped by the pedestal. Gain outside of this region is strongly negative, resulting in strong absorption of the x-ray laser. It should be noted that the longitudinal pump beam is strongly refracted in and out of the gain region, and does not propagate parallel to the target surface. In the present calculation, the density profile was assumed uniform in the z direction, to make the calculation size tolerable. Ray trace calculations show that in actual plasma, the pedestal beam will be refracted away from the target, also showing focusing with propagation due to the electron density gradient. Although the beams are curved in the high-density region, they tend to become straight at positions away from the target surface, due to the smaller density gradient. As a result, gain region with a finite width and an angle of typically 60 mrad relative to the target surface is predicted, which allows a gain length long enough for large amplification. The focusing effect can also increase the intensity of the pedestal, which is otherwise reduced due to absorption.

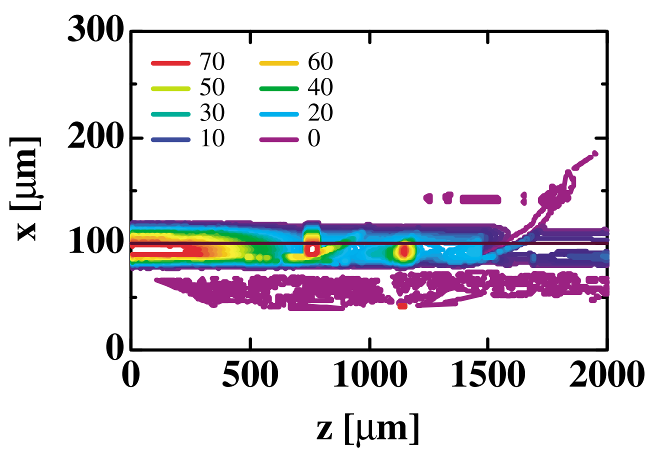

FIG. 4 (color online). Calculated spatial distribution of the 18.9 nm gain coefficient for main pump pulse with 1×10^{-5} contrast ratio. The ordinate is the direction normal to the target surface, and the abscissa is the direction parallel to the x-ray laser axis. This figure shows the gain experienced by an 18.9 nm x-ray pulse that begins propagation at $z = 0$ μm at a time 1.0 ps after the main pulse.

Another important outcome of the presence of a pedestal in the main pulse is the generation of electron density and gain distributions that have large spatial gradients. The parabolic electron density and gain profile that are produced by the pedestal are found to limit the number of transverse modes that are amplified in the grain medium. In the work by London *et al.* [15], it was numerically shown that for grain medium with such unique profiles, the efficiently guided modes that receive large amplification could be restricted to the lower order modes. Using formulations from this paper, we can calculate the number of transverse modes that receive large amplification in our experiment. Assuming that the density and gain profile is homogeneous along the x-ray laser axis, we take the lower limit of $0.18 \times gL_{\max}$ for counting the number of modes, where $gL_{\max}$ is the maximum gain-length product experienced by a single transverse mode. We take the gain-length product to be 10, which is estimated from the experimentally measured energy of our x-ray laser. If the density profile vertical to the target surface were flat, the number of effectively amplified one-dimensional Hermite-Gaussian modes would be 47, and in this case the geometrical dimensions of the gain region determines the divergence of the x-ray laser. However, this number is reduced to five for the parabolic profile predicted in our experiment, with the maximum gain obtained for the diffraction-limited transverse mode. This shows that for our experimental condition, amplification prefers transverse modes with high spatial coherence, which explains the observed small divergence.

In conclusion, an ultrasmall divergence x-ray laser has been demonstrated at 18.9 nm, based on a longitudinally pumped nickel-like molybdenum scheme. The divergence estimated from the far-field pattern of the x-ray laser beam is submilliradian, which is the smallest ever demonstrated for a TCE x-ray laser. This value is close to the 0.8 mad divergence calculated for a diffraction-limited 18.9 nm x-ray laser emitted from a 30 μm size source. The output energy of this x-ray laser is measured to be 27 nJ. Furthermore, the pump energy that is required is only 150 mJ, making it possible to operate this high performance x-ray laser at multihertz repetition rates using present-day laser technology. We have also shown using simulations that the 1×10^{-5} contrast ratio pedestal in the main pulse can result in electron density and gain profiles with large spatial gradients. These conditions are capable of the selective amplification of the lowest-order transverse mode, explaining the small divergence of the x-ray laser from such a short grain medium.

[1] J. J. Rocca *et al.*, Phys. Rev. Lett. **73**, 2192 (1994).

[2] C. D. Macchietto, B. R. Benware, and J. J. Rocca, Opt. Lett. **24**, 1115 (1999).

[3] I. A. Artioukov *et al.*, IEEE J. Sel. Top. Quantum Electron. **5**, 1495 (1999).

[4] B. R. Benware *et al.*, J. Opt. Soc. Am. B **18**, 1041 (2001).

[5] C. H. Moreno *et al.*, Phys. Rev. E **60**, 911 (1999).

[6] J. J. Rocca *et al.*, Opt. Lett. **24**, 420 (1999).

[7] J. Filevich *et al.*, Opt. Lett. **25**, 356 (2000).

[8] P. V. Nickles *et al.*, Phys. Rev. Lett. **78**, 2748 (1997).

[9] J. Dunn *et al.*, Phys. Rev. Lett. **84**, 4834 (2000).

[10] R. Li *et al.*, Phys. Rev. E **57**, 7093 (1998).

[11] R. Li and Z. Z. Xu, J. Phys. IV (France) **11**, PR2/27 (2001).

[12] J. Itatani *et al.*, Prog. Cryst. Growth Charact. Mater. **33**, 281 (1996).

[13] Y. Li *et al.*, J. Opt. Soc. Am. B **17**, 1098 (2000).

[14] J. T. Larsen and S. M. Lane, J. Quant. Spectrosc. Radiat. Transfer **51**, 179 (1994).

[15] R. A. London, M. Strauss, and M. D. Rosen, Phys. Rev. Lett. **65**, 563 (1990).